Centroiding and Point Response Function Measurements of the Mirror/Detector Combination for the X-ray Telescope of the *Swift* Gamma Ray Burst Explorer

R M Ambrosi [†a], A Abbey [‡a], I Hutchinson [a], R Willingale [a], S Campana [b], G Cusumano [c], W Burkert [d], A Wells [a], A D T Short [a], O Citterio [b], M Ghigo [b], G Tagliaferri [b], H Brauninger [d].

[a] Space Research Centre, University of Leicester, UK.; [b] Osservatorio Astronomico di Brera, Milan, Italy; [c] IFCAI, Palermo, Italy; [d] Max Planck Institut fur Extraterristrisches Physik, Garching, Germany.

ABSTRACT

The essential optical components of the *Swift* X-ray Telescope (XRT) are already developed items. They are: the flight spare x-ray mirror from the JET-X/Spectrum-X program and a MOS CCD (CCD22) of the type currently operating in orbit as part of the EPIC focal plane camera on XMM-Newton[1]. The JET-X mirrors were first calibrated at the Max Plank Institute for Extraterrestrial Physics' (MPE) Panter facility, Garching, Germany in 1996[2, 3]. Half energy widths (HEW) of 16 arc seconds at 1.5 keV were confirmed for the two flight mirrors and the flight spare. The calibration of the flight spare was repeated at Panter in July 2000 in order to establish whether any changes had occurred during the four years that the mirror had been in storage at the OAB, Milan, Italy. The results reported in this paper, confirm that the resolution of the JET-X mirrors has remained stable over this storage period.

In an extension of this test program, the flight spare EPIC camera was installed at the focus of the JET-X mirror to simulate the optical system of the *Swift* X-ray telescope. On-axis and off-axis point spread functions (PSFs) were measured and calibration data sets were used to obtain centroid positions of X-ray point sources. The results confirmed *Swift*'s ability to determine the centroid positions of sources at 100mCrab brightness to better than 1 arc second and provided a calibration of the centroiding process as a function of source flux and off axis angle.

The presence of background events in the image frame introduced errors in the centroiding process, making the choice of centroiding algorithm important. Algorithm performance and the trade-off between processing speed and centroiding accuracy were investigated.

Keywords: centroiding, point response function, x-ray, gamma ray burst, algorithm

1. INTRODUCTION

The XRT of the *Swift* Gamma Ray Burst Explorer[1] incorporates the flight spare JET-X Wolter type I set of grazing incidence mirrors and has an overall focal length of 3.5m. The telescope has an effective area of 110 cm^2 at 1.5 keV. The focal plane camera of the XRT houses the CCD22 type MOS CCD[1, 4, 5] used in the EPIC program and supplied by Marconi Applied Technologies, Chelmsford, UK. The CCD consists of 600 x 600, 40 μm pixels, with a pixel scale of 2.36 arc seconds per pixel. The energy range of the XRT is 0.2 to 10 keV and the sensitivity is 2 x 10^{-14} $erg.cm^{-2}.s^{-1}$ in 10^4 seconds[1]. In the case of the Swift XRT, an x-ray count rate of 1 count per second is equivalent to a 1mCrab source[6].

A primary goal of the *Swift* XRT is to determine the position of the x-ray afterglows of gamma ray bursts (GRB) with a maximum uncertainty of 5 arc seconds. This will be achieved approximately 100 s after the spacecraft's Burst Alert Telescope (BAT[7]) has detected a GRB and determined its position to an accuracy of 4 arc minutes. It is estimated that the

[†] Contact author rma@star.le.ac.uk, phone (+44) (0) 116 2231812, fax (+44) (0) 116 2522464, http://www.src.le.ac.uk/, University of Leicester, Space Research Centre, University Rd, Leicester LE1 7RH, UK; [‡] afa@star.le.ac.uk, phone (+44) (0) 116 2231812, fax (+44) (0) 116 2522464, http://www.src.le.ac.uk/, University of Leicester, Space Research Centre, University Rd, Leicester LE1 7RH, UK.

X-Ray and Gamma-Ray Instrumentation for Astronomy XII, Kathryn A. Flanagan, Oswald H. W. Siegmund, Editors, Proceedings of SPIE Vol. 4497 (2002)

spacecraft will take 90 s on average to reposition itself after detecting a GRB so that the XRT is able to view the GRB x-ray afterglow. This slew time will be dependent on the GRB coordinates. After the x-ray source is acquired by the XRT the CCD will be operating in an image integration mode that will be used for bright sources. The centroiding process will be carried out using the data in the first 0.1 s frame that is recorded. The estimated amount of time required to achieve a centroid position to an accuracy better than 1 arc second currently stands at 1.1 s for the RAD 6000 onboard processor.

The quick response time of the spacecraft to a GRB will allow the XRT to obtain more information about the x-ray characteristics of the GRB x-ray afterglow during the first 10^4 seconds after the event. This data would fill the gap in the observations of GRBs made to date and may provide further information about their nature, central engine and origins.

Monte Carlo simulations coupled with JET-X calibration data[1] have shown that the *Swift* XRT can obtain centroid positions of x-ray afterglows to an accuracy of less that 1 arc second and that a PSF half energy width resolution limit of 16 arc seconds could be achieved. The aim of this study was to provide further experimental verification that this centroiding goal could be achieved and how centroiding accuracy is depended on source flux, off axis angle, CCD operating mode, processing speed and choice of centroiding algorithm.

2. EXPERIMENTAL METHOD

The JET-X mirrors and the EPIC flight spare focal plane camera were mounted in the test chamber at the end of the 130 m long x-ray beam line of MPE's Panter facility. The mirrors (Figure 1) were mounted on a translation and rotation table (Figure 2) that allowed the rotation of the mirrors about the y and x axes, if we assume that the z axis is coincident with the beam line (Figure 3). At a distance of 3.5 m from the mirrors the spare EPIC flight CCD camera was mounted on a table which could be translated in x, y and z directions (Figure 4). The translation of the camera table in the z direction was used to find the focus of the mirrors and was then set at 3.5055 m. This method was used to replicate the optical system of the *Swift* XRT (Figure 3).

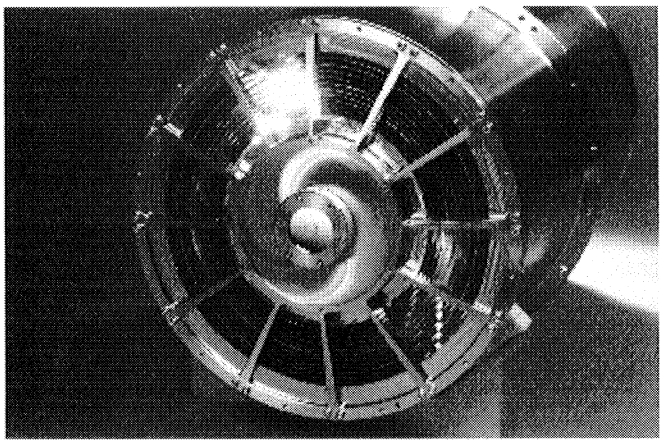

Figure 1. The JET-X flight model number 3 mirror set built by the Osservatorio Astronomico di Brera (OAB)

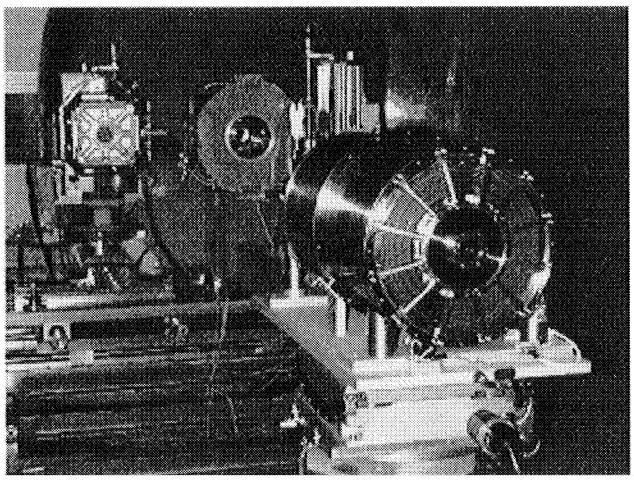

Figure 2. The JET-X mirror mounted in the Panter test chamber during the recent *Swift* XRT optical system calibration tests.

Although the objective of this calibration exercise was to obtain x-ray data at a number of energies, the data that was most of interest was that close to 1.5 keV since the effective area of the XRT peaks at 1.5 keV[1] and the calibration data quoted for the initial study carried out in 1996 is for 1.5 keV photons. Most of the calibration data was therefore taken with aluminium x-rays at 1.49 keV. Although some data was obtained with oxygen (525 eV), iron (6.4 keV) and copper (8.05 keV) x-rays, a more complete set of data at 1.5 keV was obtained. The operating temperature of the CCD was maintained at –100°C. Measurements were taken both on axis and as a function of off axis angle. The translation of the camera produced the required off axis movement of the PSF. These measurements were used to gauge how the half energy width of the PSF varies with off axis angle.

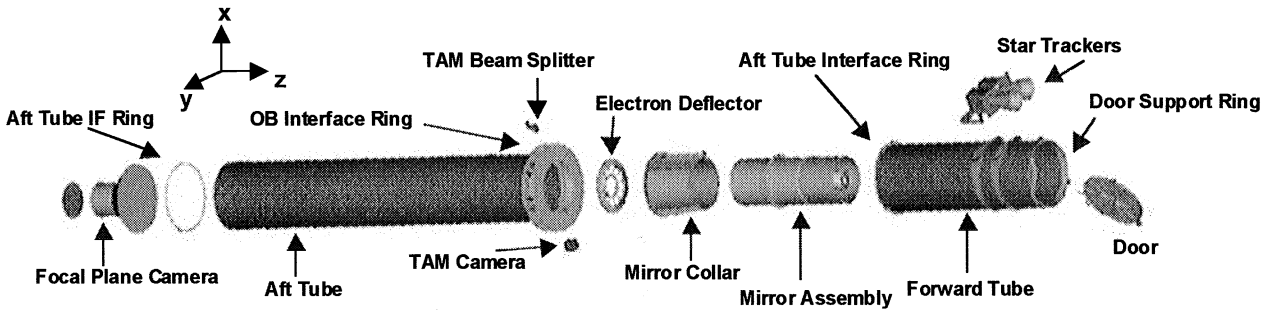

Figure 3. A schematic view of the *Swift* XRT.

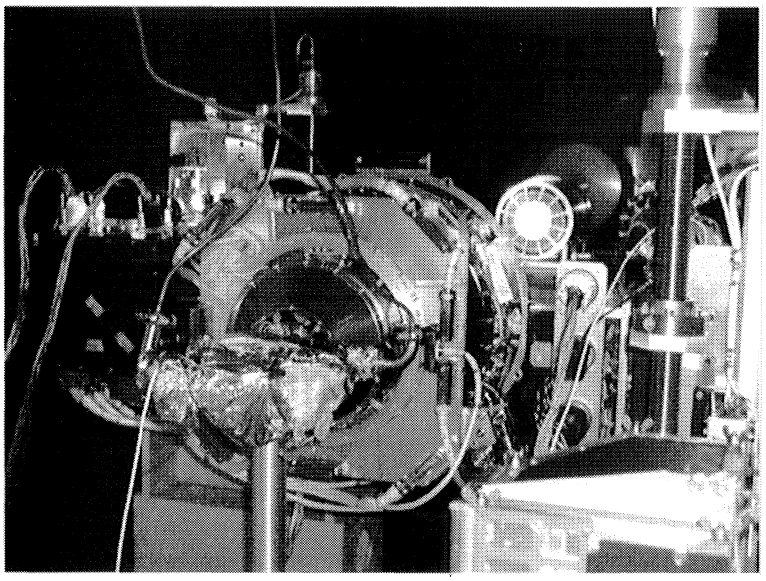

Figure 4. The spare EPIC flight camera mounted in the Panter test chamber during the recent *Swift* XRT calibration experiments. The backend of the mirrors is visible in the background at a distance of 3.5 m.

Two operating modes were used in this part of the study. The first, low gain mode, is similar to the image integrating mode that will be used by the XRT for source centroiding purposes[1] when the x-ray afterglow is in it brightest phase. The image integrating mode that will be used by the XRT is not anticipated to provide spectral information about the source due to the expected high source brightness during the initial phase of the burst and high degree of pixel saturation or pileup in the central pixels of the CCD. Low gain mode was used in combination with source fluxes of 0.7 counts.cm^{-2}.s^{-1}. The second mode of operation, high gain mode, is similar to the first mode only with a 10 fold gain increase and this was used in combination with source fluxes of the order of 0.011 counts.cm^{-2}.s^{-1}. Each data set contained 100 frames of data with an exposure time of 2.5s per frame. From this data, it was therefore possible to determine the centroiding error and PSF resolution from individual frames or look at the effect of a group of frames on the centroiding process. This was equivalent to investigating the effect of source brightness, for a particular operating mode, on centroiding accuracy and PSF resolution.

3. CENTROIDING ALGORITHM

There are many different techniques used to determine the position and intensity of discrete sources in photon images. These include relatively simple algorithms such as the centre of gravity approach and highly complex algorithms which incorporate matched filters or wavelet transforms.

The centre of gravity technique is very simple to compute but it does not take into account the shape or size of the system PSF and is therefore very sensitive to spurious features in the data such as particle events.

To avoid this problem it is necessary to either; (i) select a reduced region of pixels around the PSF in order to minimise the possibility of sampling a particle induced event, (ii) remove all of the particle events from the data before applying the centre of gravity algorithm or (iii) apply a centroiding technique which takes into account the true profile of the PSF so that the spurious events do not significantly effect the position of the centroid.

Ideally, we want to minimise the region of data that the centre of gravity is performed on. However, the position of the GRB on the detector is unknown so that the region of interest will cover the whole CCD and there will be a ~100% chance of a background event falling within this region given an estimated background count rate of 1 count.cm^{-2}.s^{-1} and a detector area of 4.5 cm^2.

One solution, is to obtain an approximate (pixel accuracy) position for the centre of the PSF by applying a matched filter to the data. In this technique, the original image is convolved with an image of the system PSF to form a secondary image. The pixel with peak intensity in this second image provides an approximate location for the centroid so that a reduced region of interest can be applied.

In general, particle induced events are removed from CCD images using an event recognition algorithm in which every pixel of the image is scanned to check the intensity levels of its neighbours. If the distribution of photons within a certain region of interest (usually a box of side 3/5 pixels) is not that expected from an X-ray then the event is rejected. In this particular case, this causes a problem because a bright x-ray source like a GRB occupies nearly all of the pixels in the core of the PSF so the source rejection algorithm rejects them.

An alternative to the centre of gravity and matched filter methods is the median filtering technique. The simplest way to do this is to fit an analytical description of the PSF to the image using a maximum likelihood technique (such as least squares) in which all of the parameters in the fit apart from the normalisation and centroid position can be frozen. However, there is a limited amount of onboard processor time with which to analyse the data (not more than one second) and the image is likely to be highly saturated in the core of the PSF so the regions of data on which to perform the least squares fitting have to be selected carefully.

Both the centre of gravity and matched filter centroiding techniques have been tested in this study and the results of this comparative exercise are shown in the next section.

4. DATA ANALYSIS AND RESULTS

4.1 Computational Method

Each 100 frame data set was broken down into 2, 4, 5, 10 and 20 frame sets or shorter exposures and a centre of gravity method was used to determine the x and y centroid positions of the PSF as a function of sampling area, source brightness and position. The half energy widths in arc seconds, the rms semi major and semi minor axes of the PSF's and the detected counts were also determined. Outputs of the spectral information contained in the x-ray data and cross section through the PSF were extracted. A typical output from the analysis of an on-axis data set is shown in Figures 5 to 7 for 100 frames of data.

The total source flux was converted into a count rate at the CCD so that the equivalent source brightness in mCrab could be determined for each data set. The average source brightness per frame was evaluated to be 180mCrab for the CCD operating in low gain mode and 10mCrab per frame in high gain mode.

The on axis x, y centroid positions, and PSF half energy widths for each short exposure were determined. Initially an arbitrary large sampling area (16 arc minutes in diameter) was selected since the initial goal was to determine whether the centroiding accuracy of less than 1 arc second could be determined and whether the PSF resolution was of the order of 16 arc seconds. The initial sampling area for the Swift XRT centroiding algorithm will be the whole CCD[8].

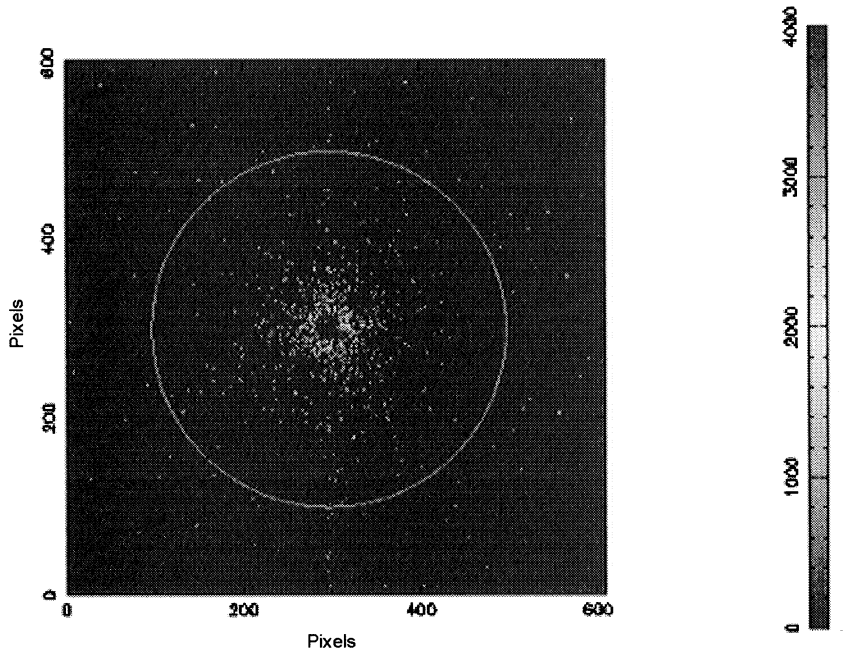

Figure 5. The point spread function produced with aluminium x-rays. The above image was produced by decoding 100 frames of x-ray data recorded with the CCD operating in low gain mode.

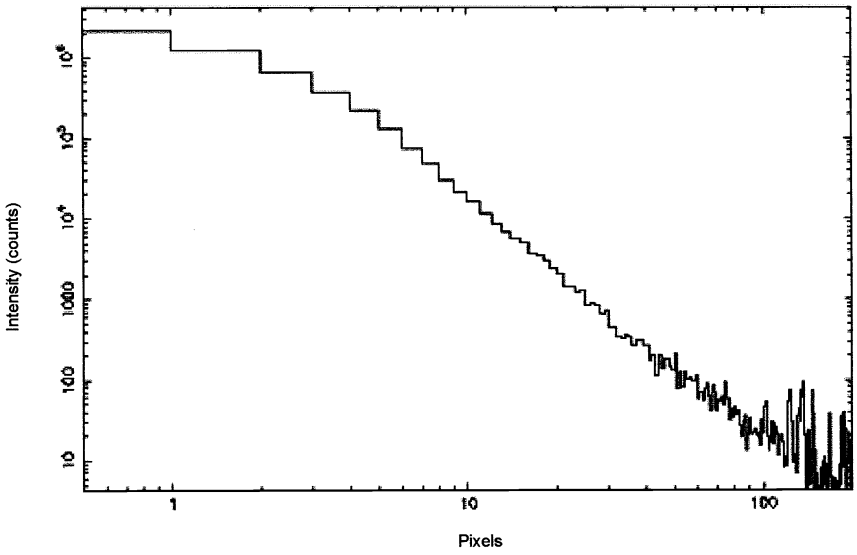

Figure 6. Line section through the PSF.

4.2 The Effect of Detected Cosmic Rays on Centroiding Accuracy and HEW Determination

A background event rate of approximately 0.05 counts per second in the Panter tank was responsible for shifting the PSF centroid positions during the centroiding process. The results depicting the x and y centroid positions for the 5 frame data set are shown in Figure 8, whereas the half energy width variation as a function of frame set number is depicted in Figure 9.

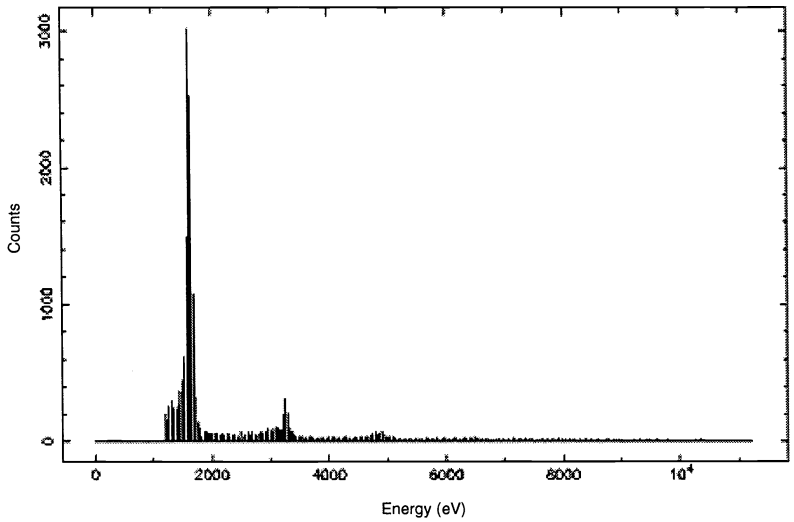

Figure 7. The pulse height distribution depicting the aluminium x-ray peak extracted from the PSF x-ray data. The effect of pileup due to the high source count rate is clearly visible.

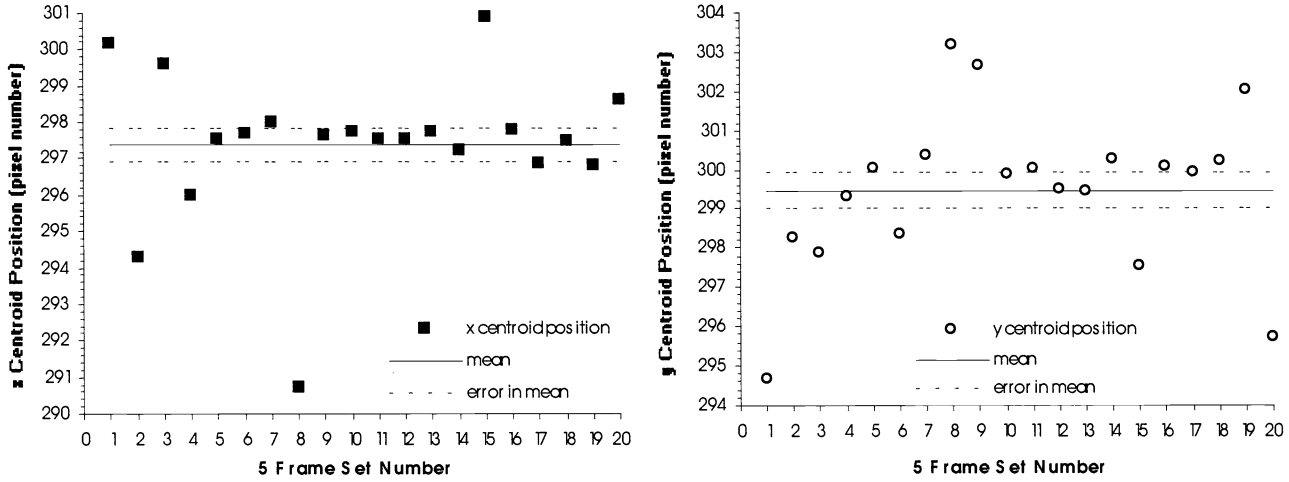

Figure 8. The variation in x and y centroid position as a function of 5 frame set number. In both cases the dotted lines define a 2 arc second error region within one standard deviation from the mean.

The interaction of muons with the CCD coinciding with the sampling area chosen for the centroiding process is clearly illustrated in Figure 10. These events are often characterised by diagonal tracks which appear much brighter than the x-ray events in the wings of the PSF. From the results shown in Figure 8, the maximum deviation in x and y centroid values from the mean is approximately 10 arc seconds, whilst the maximum deviation in the HEW values is 20 arc seconds. The mean x, y pixel co-ordinates of the PSF centroid were (297.40 ± 0.47, 299.47 ± 0.46), also the mean HEW value was 21.0 arc seconds ± 1.5 arc seconds, 5 arc seconds higher than the expected (measured) PSF resolution value of 16 arc seconds.

The error induced by these events can be removed by eliminating detected cosmic ray events from the data, reducing the sampling area of the centroiding process or by using a centroiding algorithm that does not use a centre of gravity method and that is insensitive to muonic interactions. A combination of methods would also be useful.

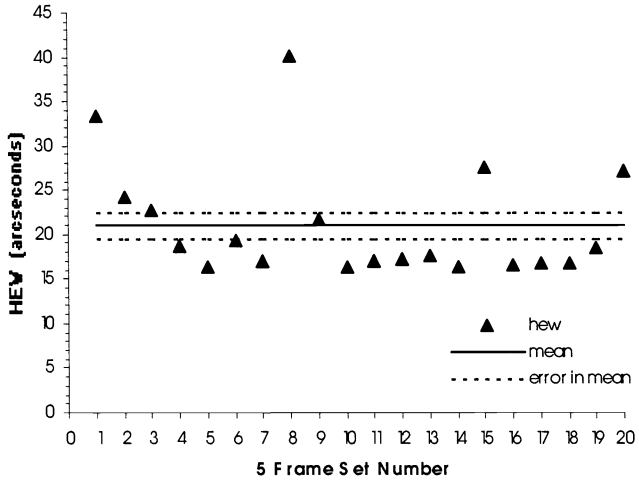

Figure 9. The variation in HEW as a function of 5 frame set number. The 1 sigma, 3 arc seconds, deviation from the mean is outlined by the dotted lines.

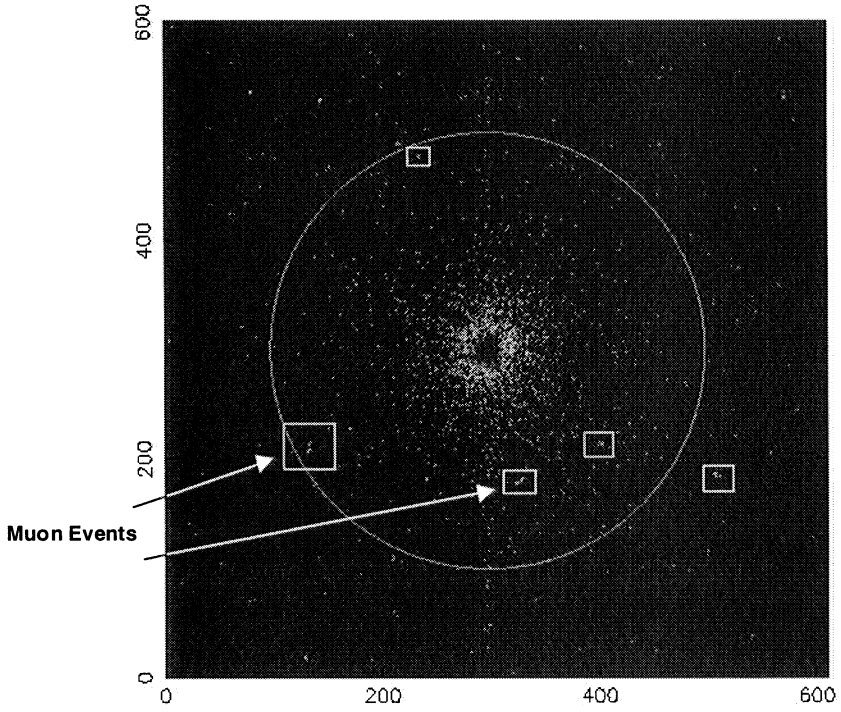

Figure 10. The point spread function produced with aluminium x-rays. The above image was produced by decoding 100 frames of x-ray data recorded with the CCD operating in low gain mode. The muon events that are responsible for the errors in the x and y centroid and HEW values are highlighted.

4.3 Improvement in Centroiding Accuracy by the Removal of Cosmic Events and Reduction in Sampling Area

The frames containing the cosmic-ray events within an 8 arc minute radius of the source were deleted from the 100 frame data set. The computational method described above was implemented again and the improvements in centroiding accuracy are shown in Figures 11 and 12. The variations in the x, y centroid and the HEW values are significantly reduced to give

mean centroid coordinates of (297.56 ± 0.063, 299.95 ± 0.069). The mean half energy width value was 16.77 arc seconds ± 0.09 arc seconds.

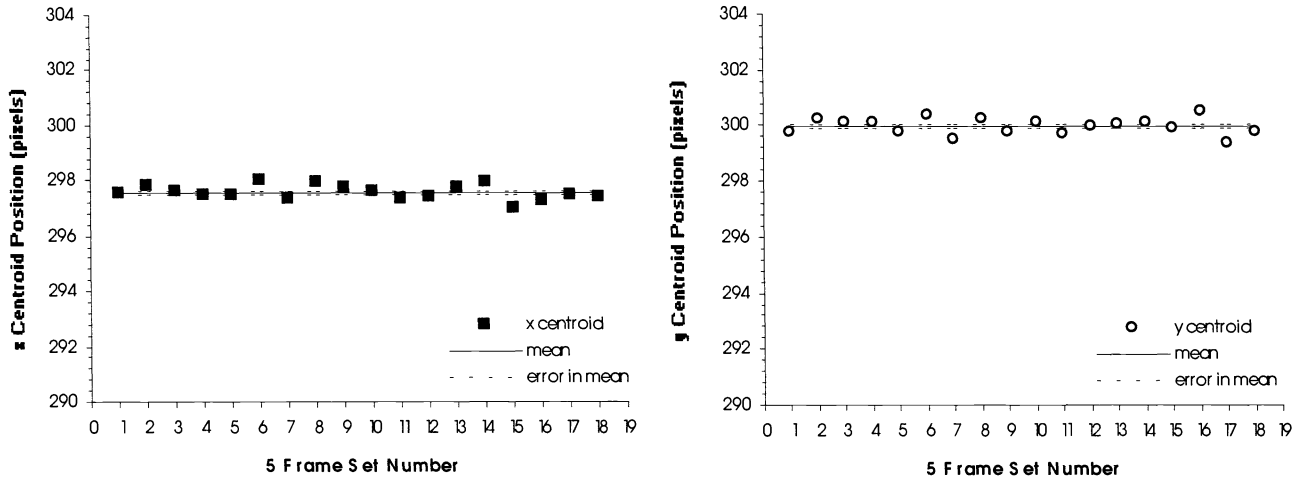

Figure 11. The reduction in the statistical variations in x and y centroid positions as a result of the removal of frames containing muon interactions with the CCD.

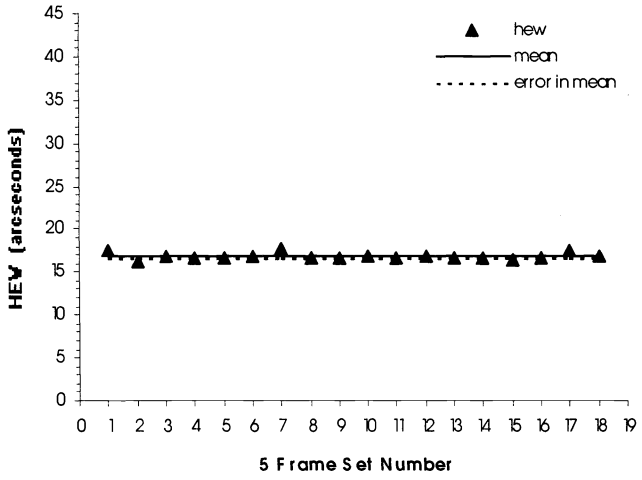

Figure 12. The removal of detected cosmic ray events from the sampling area of the centre of gravity centroiding process reduced the statistical variation in the HEW values to give a mean value of 16.77 arc seconds.

Shrinking the sampling area diameter to 4 arc minutes had a similar effect since there were no cosmic events recorded in this sampling area. The mean centroid coordinates were (297.55 ± 0.04, 300.00 ± 0.06) and the average HEW value was 16.43 arc seconds ± 0.08 arc seconds.

4.4 Centroiding Error as a Function of Source Intensity and Off Axis Angle

Each data set of n frames is equivalent to a particular source intensity in mCrab given a count rate at the detector. The centroiding error circle diameter was evaluated as a function of source intensity.

The centroiding error , σ, can be evaluated as follows:

$$\sigma = \omega_{rms} / \sqrt{N} \quad (1)$$

where ω_{rms} is the rms width of the PSF and N the number of counts [6]. The sampling area ranged between 2 arc minutes and 16 arc minutes for these calculations. In all cases the inclusion of a large portion of the wings of the PSF [6] was ensured. The on axis aluminium x-ray data was used to evaluate how centroiding error is affected by source intensity and sampling area. The frames containing muon events within an 8 arc minute radius of the PSF centroid were deleted for this investigation. The high gain data was also analysed in the same way as the low gain data in order to determine what the centroiding error range would be for sources of intensity between 10 mCrab and 150 mCrabs. The effect of reducing the sampling area and the removal of detected cosmic ray events from the data on the centroiding accuracy for bright sources is shown in Figure 13. The combined results extracted from the high gain and low gain data, where the sampling area diameter is 4 arc minutes, is shown in Figure 14. In the results shown in Figure 12, the impact of cosmic rays was removed. Equation 1 was used to produce the linear fits with ω_{rms} = 9.3 arc seconds for the high gain data and ω_{rms} = 18.8 arc seconds for the low gain data. The high gain data show that from the source count statistics a centroiding error circle radius of 0.5 arc seconds can be achieved with a count rate of 100 counts per second or a 100 mCrab source. The low gain data show that for a count rate of 1000 counts per second (1 Crab) the centroiding error circle radius is 0.3 arc seconds. This data is consistent with the original JET-X results [2] and with a study carried out by Willingale [6].

The off axis measurements were used to determine what the HEW variation with off axis angle. These results are shown in Figure 15.

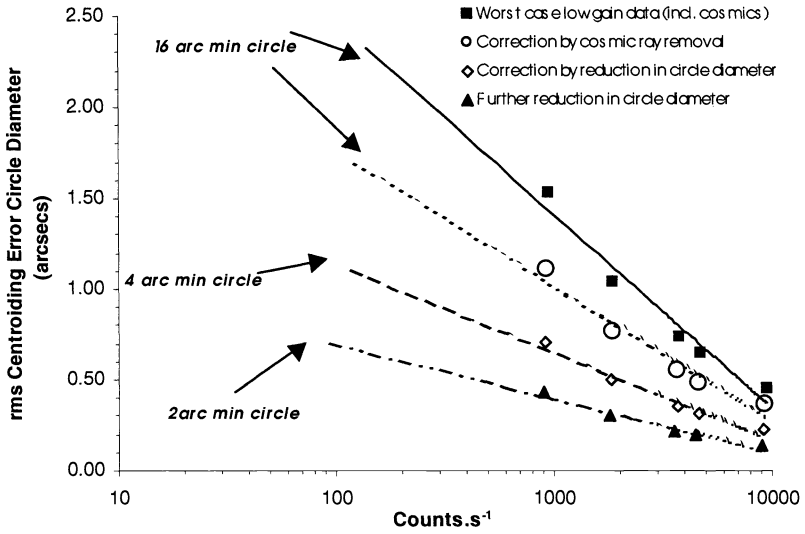

Figure 13. Improvements in the rms centroid error circle diameter as a function of source intensity due to reductions in the sampling area and removal of detected cosmic ray events from the x-ray data.

The off axis measurements show that at 7 arc minutes from the centre of the CCD there is a 7% increase in HEW. This is consistent with measurements carried out in 1996[2, 6].

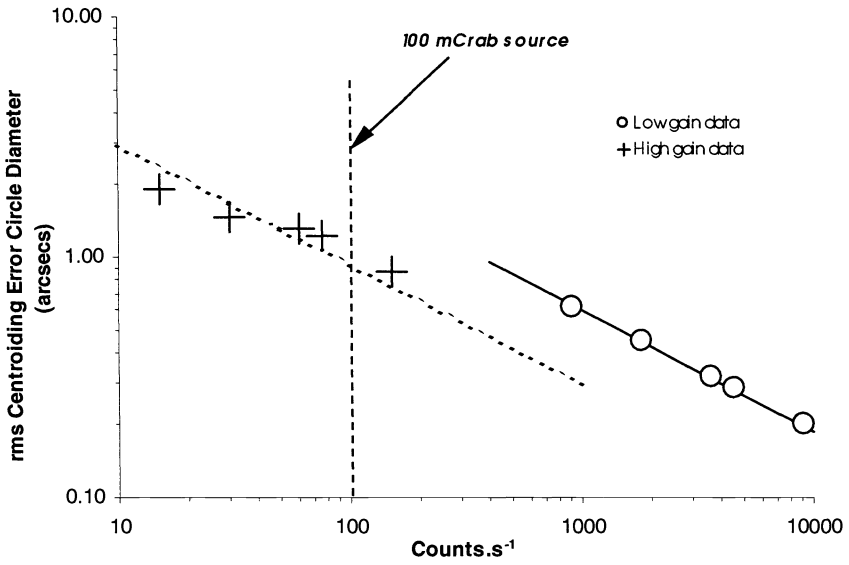

Figure 14. The rms centroiding error circle diameter as a function of source intensity for a sampling area 4 arc minutes in diameter (equivalent to the BAT error circle). Both low gain and high gain data are shown.

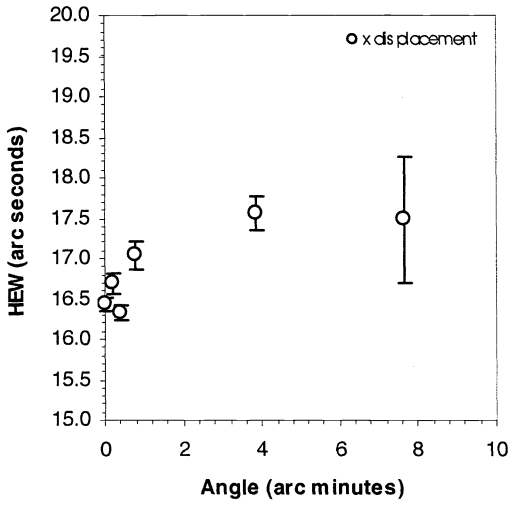

Figure 15. HEW plotted as a function of off axis angle.

4.5 Centroiding with the Matched Filter Technique

A comparison has been made between the centre of gravity method and the matched filter technique to find the centroid of the PSF with a sampling area the size of the whole CCD.

Figure 16 below shows a 2D profile of the PSF from a frame that includes a particle event. The cross shows the extent to which centroid of the image has been skewed by the counts associated with the particle. The centroid position has been shifted from the centre of the x-ray image given by the (x,y) co-ordinates (297.5, 299.5). Its new position is (304.69, 294.15), a shift of approximately 15 arc seconds in the x direction and 10 arc seconds in the y direction.

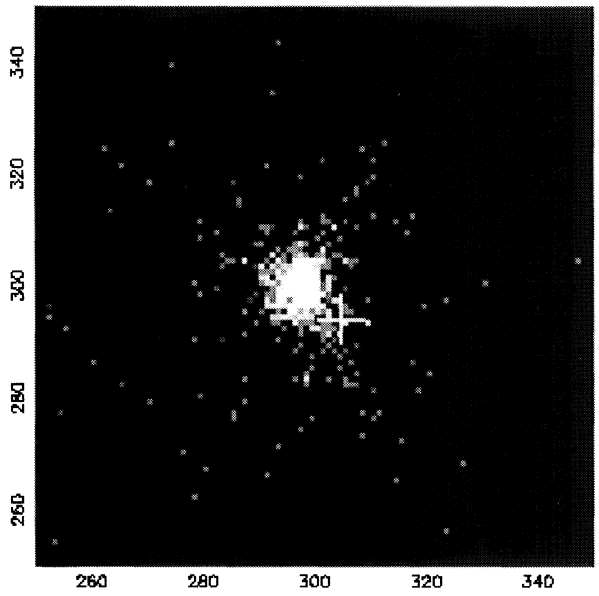

Figure 16. An expanded view of an on axis PSF produced at the Panter facility. The centre of gravity method was used to determine the centroid of the PSF which was skewed by a background event detected within 200 pixels of the centre of the CCD.

An alternative method of calculating the centroid of the PSF makes use of the matched filter technique. The centroid is calculated for an image including particle induced events by applying the matched filter. The original image is convolved with a predetermined form of the mirror PSF to form a secondary image. The pixel with peak intensity in this second image provides an approximate location for the centroid. A reduced region of interest, 100 pixels in diameter or smaller, is then selected with the provisional centroid location at its centre. This circular region corresponds to the BAT error circle (4 arc minutes in diameter). The centroid is then re-calculated for this smaller region using a centre of gravity method.

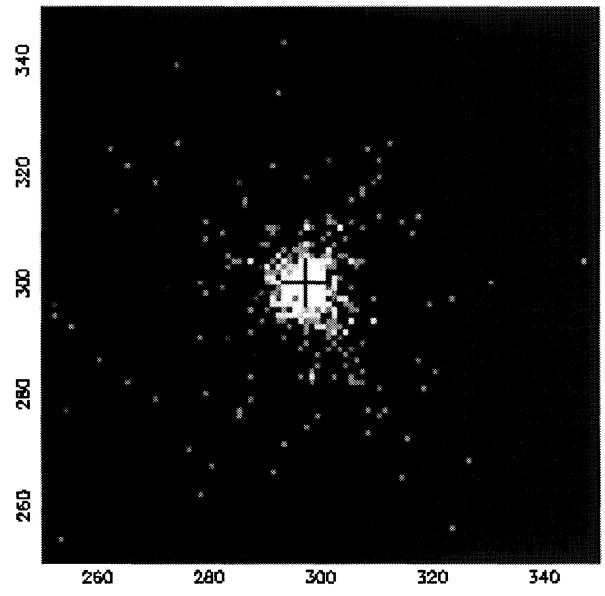

Figure 17. The use of the matched filter method resulted in a more accurate determination of the PSF centroid position.

Figure 17 shows the result of applying the centre of gravity method where the centroid co-ordinates of the PSF are determined with a greater degree of accuracy to yield an (x,y) centroid position of (297.70, 299.59).

The centre of gravity centroiding method is sensitive to the presence of detected cosmic ray events in the sampling area of the detector. With an expected background count rate in orbit of 0.15 counts per second in the BAT error circle or 4.5 counts per second over the whole CCD, the choice of algorithm is more critical, especially if the centroiding sampling area is the entire CCD. Although the deletion of these events from the data and the reduction in sampling area improve the centroiding accuracy, the matched filter technique does not require pixel association in order to obtain a comparable improvement in centroiding accuracy is shown to work effectively over a sampling area the size of the CCD. A disadvantage of using a matched filter method is that for very bright sources that produce saturated pixels in the core of the PSF, the PSF shape is degraded making it more difficult to pinpoint the PSF centroid. In such cases a modified centre of gravity method that includes pixel association may be more effective[8].

5. CONCLUSION

The results of this investigation have confirmed that the PSF of the JET-X mirror now provided for the *Swift* XRT has an HEW of 16 arc seconds. The calibration carried out in August 2000 indicated that a centroiding accuracy better than 1 arc seconds for a 100 mCrab source could be obtained with the *Swift* XRT. The implication of these results is that the storage conditions of the mirrors have not altered their response and that the *Swift* XRT requirements can be achieved.

The off axis measurements reinforce the conclusions of the previous calibration, namely that at 1.5 keV there is little variation in HEW up to 8 arc minutes from the centre of the CCD [1].

Two centroiding methods were investigated. The centre of gravity method is sensitive to background events but works for a small sampling area. The matched filter method is not sensitive to background event, it can be applied to the whole CCD and offers a viable solution to centroiding for the *Swift* XRT.

Studies to investigate source centroiding with the *Swift* XRT show that the sub 1 arc seconds centroiding accuracy for a 100 mCrab source provided that counts from background particle events can be excluded from the centroiding process. Unless background events are rejected GRB source centroid determination to the required accuracy for *Swift* will not be achieved.

ACKNOWLEDGEMENTS

The work non the Swift project is supported at the University of Leicester by the United Kingdom's Particle Physics and Astronomy Research Council (PPARC).

The authors would like to thank the Max Planck Institut fur Extraterristrisches Physik for access to the Panter calibration facility ad thei support staff for their assistance.

REFERENCES

1. D. N. Burrows, et al, "The *Swift* x-ray telescope" *Proc. SPIE* **4140**, pp. 64-75 (2000).
2. O. Citterio et al, "Characteristics of the flight model optics for the JET-X telescope onboard the SPECTRUM X-γ satellite", *Proc. SPIE* **2805**, pp. 56-65 (1996).
3. A. Wells et al, "X-ray imaging performance of the flight model JET-X telescope ", *Proc. SPIE* **3114**, pp. 392-403 (1997).
4. A. D. Holland, M. J. Turner, A. F. Abbey et al, "MOS CCDs for the EPIC on XMM", *Proc. SPIE* **2808**, pp. 414-420 (1996).
5. A. D. T. Short, A. Keay, M. J. Turner, "Performance of the XMM EPIC MOS CCD detectors", *Proc. SPIE* **3445**, pp. 13-27 (1998).
6. R. Willingale, "X-ray positioning and photometry with *Swift*", XRA Technical Study Note **XRA_RW_98_2** (1998).
7. S. D. Barthelmy, "Burst Alert Telescope (BAT) on the *Swift* MIDEX mission", *Proc. SPIE* **4140**, pp. 50-63 (2000).
8. J. Hill, private communication.